Recent Advances in Computational Convective Heat Transfer Study in a Sub-Channel for Nuclear Power Reactor and Future Directions

A. S. MOLLAH
Department of Nuclear Science and Engineering,
Military Institute of Science and Technology,
Mirpur Cantonment, Mirpur, Dhaka-1216,
BANGLADESH

Abstract: - A nuclear power reactor's primary use is to generate thermal energy, which in turn produces electricity. The primary heat source is a nuclear fission event occurring inside the fuel rod. The convection heat is transmitted through the coolant by the heat energy generated at the fuel rod wall boundary. Better heat transfer is produced in the flow area by turbulence and irregularity. As a result, turbulent flow heat transfer may present a significant challenge when predicting and assessing the thermal performance of nuclear power reactors. Computational techniques in convective heat transfer have become indispensable for solving challenging issues in the fields of science and engineering thanks to the development of current sophisticated numerical methods and high-performance computer hardware. The development of novel computational techniques and models for complicated transport and multi-physical phenomena is constantly in demand throughout applicable disciplines. This chapter's objective is to provide some recent developments in computational techniques for convective heat transfer, taking into account research interests in the community of mass and heat transfer, and to showcase relevant applications in nuclear power plant engineering domains including future directions. This study describes the most recent advancements in nuclear reactor convective heat transfer research utilizing the computational fluid dynamics (CFD) method, particularly at Ansys Fluent. This work examines the convective heat transfer and fluid dynamics fluid dynamics for turbulent flows across three rod bundle sub-channels that are typical of those employed in the PWR-based VVER type reactor. In this paper, CFD analysis is carried out using the software tool Ansys Fluent. Temperature distribution profile, velocity profile, pressure drop, and turbulence properties were investigated in this study. Boundary conditions i.e. temperature, velocity, pressure, heat flux, and heat generation rate were applied in the sub-channel domain. The main obstacles and bright spots for the CFD methods in nuclear reactor engineering are discussed, which helps to further its further uses. We intend to research a full-length fuel bundle model for VVER-1200 in the future to gather specific fluid characteristic data and use the findings to analyze safety and operate nuclear power facilities in Bangladesh. This paper presents a thorough analysis of the sub-channel thermal hydraulic codes used in nuclear reactor core analysis. This review discusses several facets of previous experimental, analytical, and computational work on rod bundles and identifies potential future directions based on those earlier studies.

Key-Words: - Computational fluid dynamics (CFD), Rod bundle, Sub-channel, VVER-1200, Convective heat transfer, Nuclear reactor, NPP, Thermal hydraulic, Test facility.

Received: April 18, 2023. Revised: September 23, 2023. Accepted: November 19, 2023. Published: December 31, 2023.

1 Introduction

Nuclear power plants (NPP) facilities in operation today are categorized as Generation III or older. Because of the relatively low operating temperatures, these NPPs are not as energy-efficient as they may be, [1]. To create the Generation IV of nuclear reactors, several nations have started an international cooperative effort. The long-term objective of creating such nuclear reactors is to raise the thermal efficiency from the existing range of 30–35% to 45–50%, [1]. Nuclear power reactors come in a variety of forms, [1]. They all share the ability to generate thermal energy, which can then be used directly, transformed into mechanical energy, and finally, in the great majority of instances, into electrical energy. Given the impact of greenhouse gases on our environment, nuclear power will contribute more to the world's energy needs in the future, [2]. A recent International Energy Outlook report, [3], claims that the need for clean energy is expected to expand by 49% between 2007 and 2035 (Figure 1). Around 440 nuclear

power stations are currently in operation around the world, while another 60 are in various stages of construction as of April 2023, [4], [5]. One hundred reactors are in a shutdown status, and several of the reactors have been operating for quite some time previously. As the globe works to reduce the damaging consequences that fossil fuels have on the environment. The existing NPPs have relatively low operating temperatures, but the future generation of nuclear power plants will have even higher thermal efficiency, increasing the production of secure electricity, [1]. Along with improved safety features, nuclear power plants' capacity is growing to lower their capital costs. More emphasis is placed on passive core cooling characteristics as a result of the nuclear accidents caused by Three Mile Island (1979), Chernobyl (1986), and Fukushima (2011). The new design of the reactors, particularly the reactor core and its accompanying systems, must take into account the lessons discovered through the studies, tests, and accidents of nuclear systems in the past. The thermal hydraulic analysis can primarily guarantee the safety of the nuclear reactor system under all core conditions, [6], [7], [8], [9]. To prevent core damage, heat must be removed from the reactor core structure at the same rate that it is generated. The reactor core is often cooled by pumping a working fluid, or "coolant," through it. Depending on the purpose of the nuclear reactor, the heat that has accumulated in the coolant is then put to use for a variety of purposes. Nuclear power reactors use the common steam cycles to convert heat into electricity. Predicting the temperature and velocity distributions in the reactor's various sections is one of the main goals of reactor thermal-hydraulics (TH), [10], [11], [12], [13], [14], [15], [16], [17], [18], [19], [20], [21], [22].

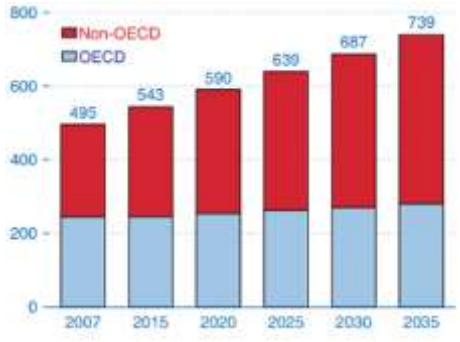

Fig. 1: Usage of energy on a global scale, 2007-2035 (quadrillion Btu), [3].

The reactor core, which generates heat and has the greatest temperatures, is the most significant component of the nuclear reactor. For varied reactor operation conditions, such temperatures must be estimated. Temperatures must be kept below prescribed safety limit values for fuel materials to ensure safe reactor operation. Predicting the stresses that the flowing coolant will impose on the reactor's interior structures is a key goal of reactor thermal hydraulics. Mechanical failures of the structures may result from excessively high or persistent oscillatory forces. As a result, the structure-mechanics analysis uses the mechanical loads in the nuclear reactor information from the thermal-hydraulic analysis to examine the integrity of the system. The impact of temperature distributions must frequently be considered in such analyses, particularly when thermal stresses are large. The reactor-physics analysis supplies information about the distribution of heat sources, whereas the former provides input data (the moderator density and other nuclear statistics not specifically mentioned here) to the thermal-hydraulic analysis. Thus, if one wishes to understand how a nuclear reactor works, it is essential to grasp thermal hydraulics (TH) characteristics. A quick change in temperature or pressure, for instance, might have serious effects on the entire system in one area of the reactor's safety analysis. TH needs to be looked at to guarantee a reactor's safe and reliable power production. However, the TH-related phenomena can sometimes be very complicated, necessitating the use of simulation techniques.

Multiphysics simulations are frequently employed because a reactor is subject to numerous different physical phenomena. These can be achieved by combining various computer codes. Researchers' diverse experimental and analytical studies of various sub-channel geometries are identified. The past research also provides perspectives for future directions. In the early phases of sub-channel thermal hydraulic analysis, the focus of research articles was mostly on analytical and experimental work done for the creation of sub-channel analysis codes, [23], [24], [25], [26], [27], [28], [29], [30], [31], [32], [33], [34], [35], [36], [37], [38], [39], [40], [41], [42]. These attempts were made to increase the accuracy of CFD predictions and to derive models from CFD for novel fuel geometries, decreasing the time needed for fuel assembly design and optimization, improving safety, and running the fewest number of tests possible to conserve resources and time. The use of the CFD technique to study rod bundle flow distributions and heat transfer is also presented in the open literature and is briefly covered in each subsection with the main conclusions and the areas that still need to be filled. This article's goal is to provide a concise review of key ideas in the subject

of nuclear thermal hydraulics as well as the various computer programs available for simulating TH-related events with the System codes (SYS-TH), sub-channel codes, and CFD codes. The final goal of this work is to use the CFD code Ansys Fluent to assess convective heat transfer in sub-channels of rod bundles and triangle tubes of VVER-type nuclear reactors, [43], [44], [45], [46], [47], [48], [49], [50]. Additionally, CFD approaches assist in obtaining the precise temperature and flow distributions within assemblies of rod bundles in square and triangle sub-channels.

2 Need for Thermal-Hydraulic Analysis in Nuclear Reactor

A nuclear power plant's central core is made up of several hundred fuel assemblies, each of which contains several fuel rods. Coolants circulate these rods or pins, picking up the heat produced by nuclear fission reactions. The safety authorities require safety assessments before granting a nuclear power plant a license, assuring the avoidance of nuclear disasters like core meltdowns and other similar events. All of the components must be designed to meet safety requirements due to this necessity. The pressure drop and heat transfer effectiveness under standard, sporadic, and accidental conditions are two technical issues in the core. Regarding the safety concern, the clad temperature is restricted. The study of thermal hydraulics and mechanics focuses on the physics and mechanics of liquid flow, energy transmission, and interactions with surrounding structures in big, intricate systems like nuclear reactors. The study of fluid flow, energy (such as heat) transfer, and interactions between fluid flow, energy, and supporting structures is known as thermal hydraulics, [6], [7], [41]. Material interactions with radioactive radiation are occasionally another crucial factor in nuclear systems. Consequently, the goals of thermal-hydraulic analysis can frequently be divided into two major groups:

a. Design: boundaries established to ensure that the plant's sturdy design can operate economically with few shutdowns and low operational expenses;
b. Safety: the bounds set forth by legal or regulatory regulations to safeguard the public's health or way of life.

3 Computer Codes for TH

Thermal hydraulics-related phenomena related to computer codes have been reviewed in this initial study, [51]. These can be classified into two primary groups, one of which is concerned with the flow's characteristics and the other with heat transfer. The most often used method in the past has been using SYS-TH codes. These rely primarily on experimental validation and make use of coarse meshes, huge control volumes, and spatial and temporal simplifications. Sub-channels are used to separate the core into these smaller, interconnected control volumes and main. Sub-channel codes, Computational Fluid Dynamics (CFD) programs, and System Thermal Hydraulics (SYS-TH) codes are the three main types of codes used for thermal-hydraulic analyses of nuclear reactors. In nuclear power facilities, large-scale phenomena are addressed with SYS-TH codes, [52]. The CFD method is most frequently used to examine particular components, and in some situations, to verify the output of SYS-TH codes. Numerous codes, including TRACE [53], CATHARE2 [54], VIPRE [55], RETRAN-3D [56], ATHLET [57], [58], COBRA [58], [59], and RELAP [60], [61] have been developed in response to the significance of thermal-hydraulic computations. A sub-channel is a flow passage established between a few or a lot of rods and the wall of the channel or shroud tube. As shown in Figure 2, either coolant-centered sub-channels or rod-centered sub-channels may be used to construct the sub-channels. The output of certain CFD simulations can then be combined with SYS-TH codes to get more precise approximations. Flow 3D [62], PorFlow [63], Flica-4 [64], Sub-chanflow [65]. Ansys Fluent/CFX [66], [67], OpenFoam [68], Comsol [69], and STAR-CCM+ [70] are a few examples of CFD programs. One of the most promising developments for reactor applications is a novel technique called computational multifluid dynamics (CMFD), which focuses on simulating two-phase flow on the mesoscale or microscale. Recent work has improved and validated CFD algorithms for two-phase/multiphase flow issues including coupling and spacer grid related to reactor safety, [71], [72], [73], [74], [75], [76], [77], [78].

4 Sub-channel Analysis for VVER Type Reactor

4.1 Reactor Description

The primary sources of nuclear electricity are light water reactors (LWRs). The pressurized water

reactor (PWR) family includes the VVER reactors, [1]. The pressurized water reactor (PWR) is by far the most prevalent nuclear system. In Figure 2, a generic PWR system is shown. A brief description of Figure 2 is given below:

- Heat is produced by the reactor vessel's core.
- Heat is transferred to the steam generator via pressurized water in the primary coolant loop (Loop 1)
- Steam is produced inside the steam generator when heat from the main coolant loop evaporates the water in a secondary loop (Loop 2). By directing the steam into the main turbine, the steam line generates energy by turning the turbine generator.
- The condenser is where the leftover steam is vented and condensed into water (Loop 3). Using several pumps, the resultant water is pumped out of the condenser, warmed up, and then fed back to the steam generator.

Electrically powered pumps circulate water to cool the fuel assemblies located in the reactor's core. The electrical grid provides power to these pumps and other facility-running systems. If off-site power is interrupted, alternative pumps that run on on-site diesel generators can provide emergency cooling water.

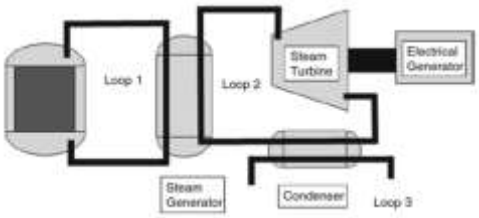

Fig. 2: Pressurized water reactor schematic

In terms of plant performance and safety, the VVER-1200/AES-2006 surpasses the VVER-1000, [79]. The Generation 3+ V-392M reactor plant design for AES-2006 is a development of prior designs employing the VVER-1000 water-cooled and water-moderated reactor, which has been successfully operated for many years. The architecture of the fuel assembly and the core shape are what separate a Western PWR from a VVER. The thermal power was increased to 3200 MWt and extra passive safety mechanisms were included to control accidents that exceed the parameters of the design foundation. There will be 1200 MWe of power produced by the VVER 1200. Both the Novovoronezh-2 location in Russia and the Rooppur site in Bangladesh are actively working on the building of a VVER-1200, [79]. The pressurized water-moderated VVER-1200/AES-2006 reactor has 163 fuel assemblies. In addition to the 312 fuel rods, each fuel assembly has 18 directing channels for control rods or burnable poisons. A single rod is used to represent the typical behavior of all the fuel rods in each channel when modeling the fuel rods, and the individual sub-channels are pooled to produce an equivalent flow area in the core analysis. The reactor coolant system circulates coolant in a closed circuit to transmit heat from the reactor core to the secondary side of the reactor. Figure 3 depicts a schematic illustration of the nuclear reactor's flow routes, [1].

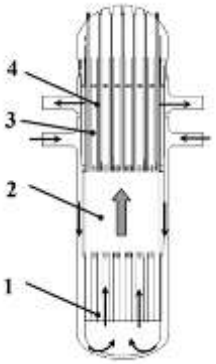

Fig. 3: Flow path diagram for PWR, [1]

Coolant is transported from intake connections to the perforated reactor bottom via a double-walled downcomer, where it rises to the reactor vessel. After flowing through the lower lattice and perforated bottom (1), the stream is divided into control bundle channels and 312 operational fuel channels of the active core (2). After leaving the working fuel bundle channels, the heated stream enters the mixing chamber (3). It then moves via apertures in the guide tubes' walls to the mixing chamber through the control bundle channels and guide tubes (4). The reactor coolant system is made up of a reactor, a pressurizer, and four circulation loops. Each of these loops has a steam generator, a reactor coolant pump set, and major coolant pipelines that connect the loop equipment to the reactor. Between the primary and secondary sides is a steam generator. Figure 4 depicts the fuel assembly model, [1]. Table 1 presents the primary side's major design and thermal-hydraulic performance during the reactor plant normal operation.

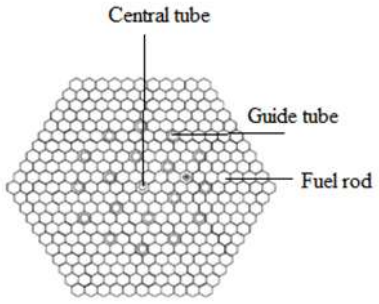

Fig. 4: VVER-1200 assembly configuration, [48]

The FAs are made to generate heat and transmit it from the fuel rod surface to coolant over the course of their intended service life while staying within the permitted design parameters for fuel rod damage. The FAs have a nominal height of 4570 mm. The height of the fuel rod's power-generating portion in the hot state of the reactor is 3750 mm. A tube made of zirconium alloy covers the fuel rod. Inside the cladding are stacked sintered UO_2 pellets with a 5% (4.95%) maximum enrichment. Ceramic uranium dioxide (UO_2) pellets with a melting point of 2800 °C serve as the fuel. The VVER-1200 core is constructed using four distinct enriched fuel types (1.6%, 2.4%, 3.6%, and 4.95%). The cylindrical pellets are then placed into helium-filled tubes made of a corrosion-resistant zirconium metal alloy containing 1% Nb to help with heat conduction. An average fuel rod produces 167.8 W/cm of linear heat.

Table 1. Thermal hydraulic parameters, [48]

Parameter	Value
Reactor nominal thermal power, MW	3300
Coolant inventory in the reactor coolant system , m^3	290
Coolant inventory in PRZ at nominal power operation, m^3	55
Primary pressure at the core outlet, absolute, MPa	16.2
Coolant temperature at reactor inlet, ^oC	298.2
Coolant temperature at reactor outlet,^oC	328.9
Coolant flow rate through rector, m^3/h	86000
Primary side design parameters: -gauge pressure, MPa -temperature, ^oC	 17.64 350
Pressure of the primary side hydraulic tests, MPa -for tightness; -for strength	 17.64 24.5

A sub-channel in a nuclear reactor is a section of the fuel assembly that is enclosed by fuel rods. The long, cylindrical tubes that contain the nuclear fuel pellets are called fuel rods. The heat from the fuel rods is transferred to the coolant as it passes through the sub-channels. The size and shape of the sub-channels, which are distributed in a regular pattern throughout the reactor core, are determined by the reactor's design and operational conditions. The thermal-hydraulic behavior of sub-channels is an important consideration in the design and operation of nuclear reactors. Therefore, reactor operators continuously monitor the sub-channel temperatures and coolant flow rates to ensure the safe and efficient operation of the nuclear reactor. In cross-section, reactor core fuel assemblies can be square, hexagonal, or circular as depicted in Figure 5.

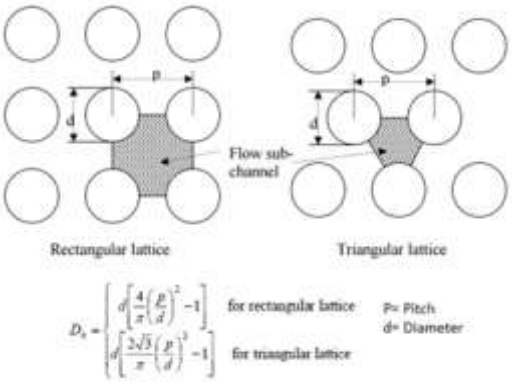

Fig. 5: An example of a sub-channel, [10]

Rod diameter, rod-to-rod pitch (p), type, and position of rod gaps, as well as, for arrays within shrouds, the distance between the rods and the shroud as well as the geometry of the shroud, are the key elements that determine the thermal-hydraulic performance of rod bundles. Radial and axial variations in the fuel rod power output also cause significant variations in the array's coolant flow rate and thermal coolant conditions. A 1200 MWe nuclear power reactor's hexagonal fuel sub-assembly underwent a 3D CFD analysis for turbulent flow in the interior, edge, and corner sub-channels. Since the three sub-channels geometrical forms and boundary conditions varied, so did the effects of the operational parameters. The findings may be used to support the following observations, [48]:

1) When compared to the other two sub-channels, the corner sub-channel has much higher turbulent attributes such as turbulent kinetic energy, turbulence dissipation rate, and turbulent eddy viscosity over the axial length. This eddy viscosity

causes the flow velocity in the corner sub-channel to drop.
2) The fluid temperature is lower at the edge sub-channel region than in the other two sub-channels due to the larger Nusselt Number there. However, the corner sub-channel has a higher chance of DNB and the creation of a hot spot in the fuel rod next to it than the other two sub-channels due to a falling Nusselt number and increasing temperature and fluid enthalpy along its axial length.
3) The length of the fuel sub-assembly should be such that the Nusselt number can achieve its fully developed state to ensure proper heat evacuation from the fuel rod surface. In this simulation, the edge and interior sub-channels both reach the fully developed Nusselt number. Here, the algorithm should more than take into account the length of the fuel subassembly to find a fully developed Nusselt number in the corner sub-channel.
4) The increase in friction factor slope is greater at the corner sub-channel along the direction of fluid flow because there is higher turbulent viscosity there. Because the coolant flow area is larger near the edge, the friction factor is higher.
5) In all three sub-channels, the relative pressure decrease is virtually constant for different Reynolds numbers.

4.2 Thermal Hydraulic Analysis of the Sub-channel

The behavior of the coolant and fuel rods in the sub-channel under various operating conditions is investigated as part of the thermal-hydraulic analysis of a sub-channel of a VVER-1200 reactor fuel assembly. The geometry of the VVER sub-assembly results in three different types of sub-channel meshes: triangular (interior sub-channel) over the bulk of the bundle, edge sub-channel, and corner sub-channel, as shown in Figure 6, [48].

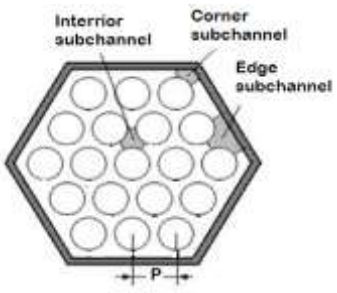

Fig. 6: Sub-channels of the fuel sub-assembly of VVER-1200 reactor

Calculating several parameters, such as the coolant's flow rate, temperature, pressure, and heat transfer coefficient as it travels through the fuel assembly sub-channel, is covered by the study. Nuclear processes inside the fuel rods produce heat, which is delivered to the coolant via the cladding and coolant gap. The heat transfer coefficient determines how effectively heat is transferred between the coolant and the fuel rods. A thermal hydraulic analysis of a sub-channel in the fuel assembly of a VVER-1200 reactor is required to guarantee the safe and efficient operation of the reactor. It aids in the detection of potential issues and the optimization of the reactor's design and operational parameters to improve both its usability and safety.

Turbulent flow is a type of fluid flow in which the fluid moves in an irregular and chaotic manner, with fluctuations in velocity and pressure occurring randomly in both time and space. This type of flow occurs when the fluid is moving at high velocities or when the flow encounters obstructions or irregularities in the channel or pipe. Turbulent flow is characterized by high Reynolds numbers (Re>4000), which indicate that the inertial forces in the fluid are much larger than the viscous forces. In turbulent flow, the fluid particles move in a complex, three-dimensional pattern, with eddies and vortices forming and breaking down randomly Table 2 contains a listing of the VVER-1200 reactor's boundary conditions as well as its operating temperature and pressure, [48].

Table 2. Boundary conditions for sub-channel model

Parameters	value
Pressure at the inlet boundary	16.2 MPa
Velocity at the inlet	5.66 m/s
The temperature at the inlet	571.2K
Hydraulic diameter	0.0162 m
Heat flux at the wall	2135 W/m^3
Heat generation rate at the wall	293475 W/m^2

The general CFD methodology employed in the current investigation is presented in Figure 7 in the form of a self-explanatory flow chart.

The Ansys Fluent code is used to solve each of these equations. Two numerical approaches have been used in Ansys Fluent:
• solver depending on pressure
• solver based on density

The density-based technique was primarily employed for high-speed compressible flows, whereas the pressure-based approach was created for low-speed incompressible flows. Recently, both approaches have been improved and recast to address problems and work for a variety of flow situations outside of their original or conventional meaning.

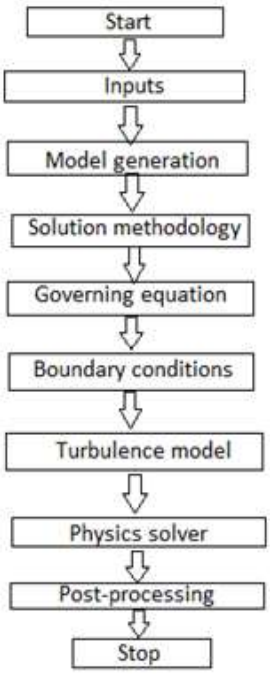

Fig. 7: A flow chart describing the analysis's overall methodology

The momentum equations are used in both techniques to determine the velocity field. The density field is obtained using the continuity equation in the density-based approach, whereas the pressure field is derived using the equation of state. According to the assumptions of a steady, incompressible flow, the differential equations governing flow, turbulence, and heat transfer are as follows, [47]:

Continuity Equation:

$$\nabla . (\rho \vec{u}) = 0 \quad (1)$$

Conservation of momentum:

$$\rho (u . \nabla)u = \nabla . [-pI + (\nabla u + T (\nabla u))(\mu t + \mu) - \frac{2}{3} (\nabla . u)I(+ \mu t) - \frac{2}{3}\rho kI] + F \quad (2)$$

Conservation of energy:

$$\nabla . [\vec{u}(\rho E + p)] = \nabla . [k_e \nabla T - \sum_j h_j \vec{J_j} + (\bar{\bar{\tau}}_e . \vec{u})] \quad (3)$$

Where k_e is the effective conductivity and k_e is the turbulent thermal conductivity defined according to the turbulence model being used. The first three terms on the right hand side of Eq. (3) represent energy transfer due to conduction, species diffusion, and viscous dissipation, respectively, [47].

Heat Transfer in Fluid:

$$\rho CPu . \nabla T = \nabla . (K \nabla T) + Q + Q_{vh} + Wp \quad (4)$$

Turbulent kinetic energy equation:

$$\rho (u . \nabla) k = \left[\left(\mu + \mu \frac{t}{\sigma k} \right) \nabla k \right] . \nabla + Pk - \rho \varepsilon \quad (5)$$

Specific dissipation rate equation:

$$\rho (u . \nabla) \varepsilon = \nabla . [(\mu + \mu_t / \sigma_e) \nabla \varepsilon] + C_{e_1} \frac{\varepsilon}{k} P_k - C_{e_2} \frac{\varepsilon^2}{k} \rho \quad (6)$$

Turbulent Eddy viscosity:

$$\mu t = \rho C\mu (k_2 / \varepsilon) \quad (7)$$

Where values of constants in the k-ε turbulence model are:

C_μ= 0.09; C_{e1}= 1.44; C_{e2}=1.92; σ_k=1.0; σ_e = 1.3.

Ansys 2021R1 is the numerical simulation tool utilized in this work. Establishing governing equations, boundary conditions, and initial conditions are typically steps in the process of creating a mathematical model. The standard principles of conservation in physics, such as mass conservation, momentum conservation, and energy conservation, apply to generic fluid movement. These conservation laws are expressed mathematically in the governing equation. The continuity equation and the momentum equation can be utilized directly as the governing equations if there is no heat exchange in the fluid flow inside the hydraulic turbine. The differential equation related to the numerical solution is as follows:

Governing equation
Continuity equation:

$$\partial \rho / \partial t + \partial / \partial (\rho u_f) = 0 \quad (8)$$

Since the density of an incompressible fluid, ρ, is constant across time ($\partial \rho / \partial t$=0), the continuity equation for that fluid can be reduced to the following differential form.

$$\partial u_j / \partial x_j = 0 \quad (9)$$

Universal momentum equation:

$$\partial u_i / \partial t + (\partial u_i / \partial x_j) = f_i + 1/\rho (\partial \tau_{ij} / \partial x_j) \quad (10)$$

The constitutive relation
$\tau_{ij} = (\partial u_i / \partial x_j + \partial u_j / \partial x_i) - p\delta_{ij} - (2/3)\ \mu\ (\partial u_k / \partial x_k)\ \delta_{ij}$
of Newtonian fluid is substituted into the above equation.

$$\partial ui/\partial t+\partial/\partial x(uiuj)=f_i-(1/\rho)(\partial p/\partial x_i)+(\mu/\rho)(\partial^2 u_i/\partial x_j\partial x_j)+(1/3)(\mu/\rho)(\partial/\partial x_i)(\partial u_k/\partial x_k) \quad (11)$$

The momentum equation may be further reduced for incompressible fluids, where the continuity equation necessitates $\partial u_k/\partial x_k=0$.

$$u_i/\partial t+\partial/\partial(u_iu_j)=fi-(1/\rho)(\partial p/\partial x_i)+(\mu/\rho)(\partial^2 u_i/\partial x_j\partial x_j) \quad (12)$$

where t is the mass force on the unit mass fluid, τij is the stress tensor, δij is the second-order unit tensor, ρ is the fluid density, is the pressure, and t is the time.

The turbulence equation must be included since the flow in a hydraulic turbine is typically turbulent. The standard k-ε model, RNG k-ε model, and Realizable k-ε model are often used CFD turbulence models in Fluent fluid analysis. To varied degrees, the three k-ε models can reproduce the features of fluid flow; nevertheless, when powerful swirl flow and curved streamline flow are simulated, the Standard k-ε model exhibits distortion. Like the RNG k-ε model, the Realizable k-ε model can be used for numerical calculations of different kinds of fluid flows and offers advantages in swirl flow prediction. The water flow in the nuclear reactor's sub-channel is simulated using the Realizable k-ε model. Here are the k-ε equations displayed.

$$\partial/\partial(\rho k)+\partial/\partial x_i(\rho u_i k)=\partial/\partial x_j[(\mu+\mu^t/\sigma_k)(\partial k/\partial x_j]+G_k-\rho\varepsilon \quad (13)$$

$$\partial/\partial(\rho\varepsilon)+\partial/\partial x_i(\rho u_i\varepsilon)=\partial/\partial x_j[(\mu+\mu_t/\sigma_\varepsilon)(\partial k/\partial x_j)]+\rho C_1S_\varepsilon-C_2\rho\{\varepsilon^2/(k+\sqrt{v\varepsilon})\} \quad (14)$$

Where$\mu_t=(k^2/\varepsilon)$, $G_k=\mu_tS^2$, $C_1=\max(0.43,\eta/(\eta+5))$, $\eta=S(k/\varepsilon)$, $S=\sqrt{(2S_{ij}S_{ij})}$, $S_{ij}=1/2(\partial u_i/\partial x_j+\partial u_j/\partial x_i)$

The formula mentioned above has the following values: t = fluid density (d), k = turbulent kinetic energy, d = dissipation rate, d = dynamic viscosity, and v = coefficient of kinematic viscosity. The coordinate components are xi and xj; the speed in the direction of i and j, respectively, is denoted by ui and uj (i, j = 1, 2, 3); the word responsible for producing turbulent kinetic energy due to average velocity is Gk. S represents the tensor coefficient for average strain rate; k and ε's Prandtl numbers are σk and $\sigma\varepsilon$, respectively; The turbulent viscosity coefficient is denoted by V_t; The turbulent field (k and ε), the rotation rate, average strain, and the system's angular rate of rotation all influence $C\mu$; the model coefficient is C1, and the constants are σ_k = 1.0, σ_ε = 1.2, and C_2 = 1.9.

The two conveyed variables in the k ، turbulence model are the rate of dissipation of the turbulent kinetic energy, ε, and the energy itself; k. Fluent employed the following equations in the conventional k- ϵ model, [66]:

$$\frac{\partial}{\partial t}(\rho k)+\frac{\partial}{\partial x_i}(\rho k u_i)=\frac{\partial}{\partial x_j}\left(\left(\alpha_k\mu_{eff}+\frac{\mu_t}{\sigma_k}\right)\frac{\partial k}{\partial x_j}\right)+G_k+G_b-\overline{\rho}\varepsilon-Y_M+S_k \quad (15)$$

and,

$$\frac{\partial}{\partial t}(\rho\varepsilon)+\frac{\partial}{\partial x_i}(\rho\varepsilon u_i)=\frac{\partial}{\partial x_j}\left(\left(\alpha_\varepsilon\mu_{eff}+\frac{\mu_t}{\sigma_\varepsilon}\right)\frac{\partial\varepsilon}{\partial x_j}\right)+C_{1\varepsilon}\frac{\varepsilon}{k}(G_k+C_{3\varepsilon}G_b)-C_{2\varepsilon}\rho\frac{\varepsilon^2}{k}+S_\varepsilon \quad (16)$$

where α_k and α_ε are the inverse effective Prandtl numbers for k and ε, respectively, which are computed variables that Fluent uses to modify μ_{eff}, μ_{eff} is the effective dynamic fluid viscosity.

It is anticipated that the SST k-ω model will yield more precise and dependable predictions for a larger class of flows by utilizing the k-ω model in the near wall region and the k-ε model for the free stream zone [66]. The SST k-ω model makes use of the following transport equations, [66]:

$$\frac{\partial}{\partial t}(\rho k)+\frac{\partial}{\partial x_i}(\rho k u_i)=\frac{\partial}{\partial x_j}\left(\Gamma_k\frac{\partial k}{\partial x_j}\right)+G_k-Y_k+S_k \quad (17)$$

$$\frac{\partial}{\partial t}(\rho\omega)+\frac{\partial}{\partial x_i}(\rho\omega u_i)=\frac{\partial}{\partial x_j}\left(\Gamma_\omega\frac{\partial\omega}{\partial x_j}\right)+G_\omega-Y_\omega+D_\omega+S_\omega \quad (18)$$

where Y_k and Y_ω represent the turbulence-induced dissipation of k and ω, Dω is the cross-diffusion term, G_ω is the production of ω, and G_k and Gω are the effective diffusivity of k and ω.

Boundary conditions, such as wall boundary conditions, import and export boundary conditions, etc., are necessary for the control equations to have a conclusive solution. The correctness of the computation results is directly impacted by the choice of boundary conditions.

Fluent discretizes the governing equations using the finite volume method. Its main concept is as follows: a non-repetitive control volume surrounds each grid point in the calculating region, which is separated into grids. A set of discrete equations is obtained by integrating the governing equations over each control volume. The discrete equations in this paper were interpolated using the second-order upwind scheme, closed using the Realizable k-ε turbulence model, and solved with pressure and

velocity coupling using the Semi-Implicit Method for Pressure Linked Equations (SIMPLE) algorithm. For the purpose of studying the sub-channels with coolant as a water channel within, which removes heat from the fuel rods and transfers it to the steam generator, the flow pattern is turbulent in nature. In the fluid domain, steady-state heat transfer is maintained in addition to forced convection flow analysis. Construction of the computational domain is done using ANSYS 21. The ANSYS 2021 R1 geometry module is used to create the center, edge, and corner sub-channel geometries. Figure 8 represents the center, edge, and corner sub-channels geometry that is used in this study, [48].

4.2.1 Subchannel Geometry

Depending on the core geometry, the sub-channel can have either a square or a triangular shape. A group of connected sub-channels that are part of a simulated rod bundle are thought to contain a one-dimensional flow. Through cross-flow mixing, the channels are connected, [48]. Compared to SYS-TH codes, the meshing utilized in sub-channel codes is more precise. We need to take geometrical simplification into consideration in many nuclear thermal-hydraulic problems. The geometry is highly essential since it affects the boundary condition in the CFD calculation, unlike the system code where geometry-related information must be provided by the code user in an averaged fashion. The mesh has a significant role in the precision of the calculated findings. However, because it has limitless degrees of freedom, it is difficult to directly compare to other mesh configurations and represents geometry quantitatively. The user-supplied nodalization utilized in system codes is replaced by grid generation techniques in the CFD approach. Geometrical data, such as the pressure drop coefficient, is frequently provided as an average in the system codes. This strategy may be troublesome since the geometry has an impact on the boundary conditions, which are crucial to CFD computations.

4.2.2 Generation of Mesh

Mesh generation comes next, after geometry creation. The Ansys fluent mesh tool was used to generate mesh for each of the three different geometrical models (different sub-channels). Similar to meshing in finite element simulations, the development of a mesh in CFD simulations affects the simulation's accuracy and processing time. The mesh generated by the problem's grid generation approach will attempt to fit the geometry of the system under simulation. Ansys's meshing capability reduces the time and effort needed to get precise results.

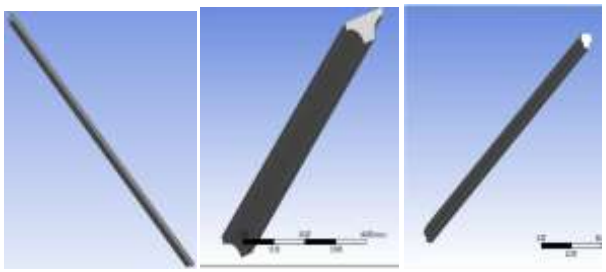

a. Center Sub-channel b. Edge Sub-channel
c. Corner Sub-channel

Fig. 8: Geometry of 3 sub-channels

Ansys contributes by developing more automated and improved meshing tools because meshing frequently consumes a significant portion of the time required to achieve simulation results. The elements take inflation at the model's borders and are orientated during the mesh production of tetrahedral structures. A properly defined turbulence velocity profile requires a domain length of 3.75 m, which is 10% of the total heat generated by the fuel rod and long enough to produce the desired pattern. The geometry and mesh were created via the ANSYS 2021R1 program. Figure 9, Figure 10 and Figure 11 shows outlet mesh, center sub-channel whole domain mesh, edge sub-channel whole domain mesh, and corner sub-channel whole domain mesh receptively.

A cell's stretching is gauged by its aspect ratio. The distances between the cell centroid and face centroids and nodes are two examples of the distances that are used to compute it. The ratio of the greatest value to the minimum value of any of these distances is used to calculate it. Below are some tetrahedral mesh statistics, including skewness, aspect ratio, orthogonal quality, and y+:

Average Skewness: 7.89×10^{-2} (Range: 3.786×10^{-6}-0.7)
Orthogonal quality: 0.9654 (Range: 0.783-1.000)
Aspect ratio: 19.876 (Range: 3.783-68.238)

Aspect ratios of other elements are computed from the aspect ratio of a perfect tetrahedral element. When normalized concerning a perfect tetrahedral, the aspect ratio of an element is the ratio of its longest edge to the shortest normal dropped from a vertex to the opposite face. The aspect ratio of a perfect tetrahedral element is 1.0 by definition. To assess the mesh quality, the Ansys software software computes the aspect ratio. The majority of the parts in a high-quality mesh have an aspect ratio of fewer than five. This study's aspect value ranges from 3.783-68.238), with an average value of

19.876. This value agrees well with the values seen in the literature, [25].

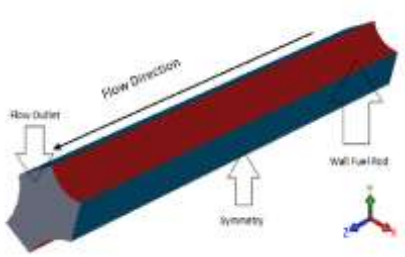

Fig. 9: Demonstration of computational geometry, [43]

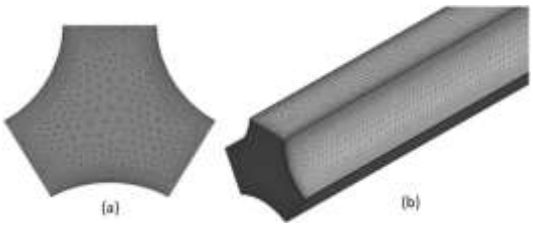

Fig. 10: Tetrahedral grid generation over the geometry (Centre sub-channel), [43]

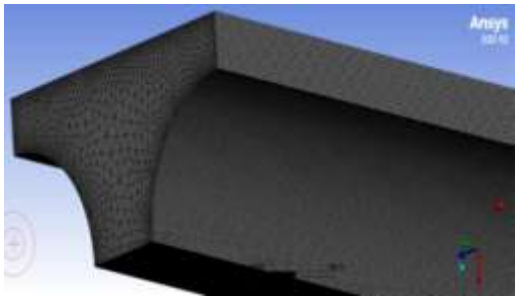

(a)

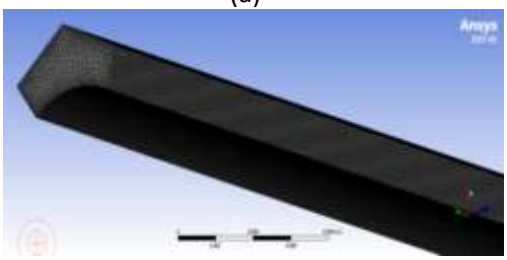

(b)

Fig. 11: a) Edge sub-channel mesh and b) Corner sub-channel mesh, [48]

For the convergent solutions, the residual value of the energy equation is set to be 10^{-8}, the residual value of the momentum equation, k, and ε equations to be 10^{-6}, and the residual value of the continuous equation to be 10^{-4}. The number of grids that meet the convergence requirement is about $4.8x10^6$. Several mesh sizes were investigated for this purpose, and the convergence criterion was very well satisfied at $4.8x10^6$. The residuals of every equation were tracked, and the behavior graph for each is displayed in Figure 12. After 3000 iterations, every chosen truncation criterion was met, with the continuity equation criterion being the first. With a quick beginning decrease and a less steep rate in the final iterations, the residual reduction reported by other authors, [43], [44] is obtained for all equations.

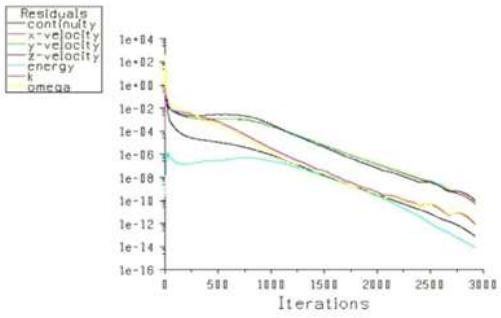

Fig. 12a: Residual values vs iteration with $4.8x10^6$ meshes

It is also appropriate to monitor the drag coefficient to examine convergence, as stated in the fluent user handbook [66]. The value of this coefficient has not changed much since the thirtieth iteration, as seen in Figure 12b, indicating solution stability [66].

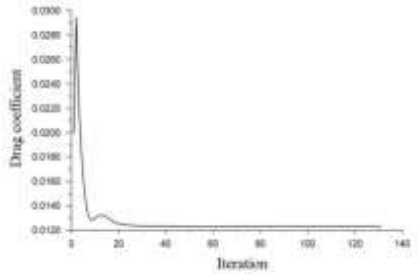

Fig. 12b: Drag coefficient for every cycle

4.2.3 Boundary Conditions

The solid surface walls of the fuel rod claddings do not slip or have a smooth boundary condition for the flow computations in the domains. The constraint was put on the symmetry planes in the symmetries. The sub-channels lower portion and top surfaces were configured as periodic interfaces, which aid in simulating the flow in situations with fully developed turbulent flow. That is shown in Figure 13, [48].

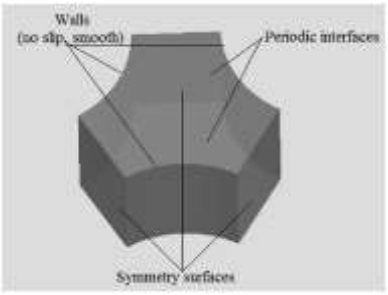

Fig. 13: Boundary conditions of center sub-channel, [48]

The mass flow rate utilized as the entrance velocity for the sub-channels is 5.66 ms^{-1}, and the Reynolds number Re = 3.75×10^4 is determined from Equation (8).

$$Re = (\rho u D_h)/\mu \quad (8)$$

Where, ρ = Density of the fluid (g/cc); u = Velocity (m/sec); D_h = Hydraulic diameter (m); μ = Viscosity (Pa.s).

The non-dimensional Nusselt number, Nu, is utilized to directly assess the heat transmission characteristics. Equation (9) gives Nu's definition.

$$N_u=\frac{hD_h}{k} \quad (9)$$

Where, h is a convective heat transfer coefficient ($W/m^2.K$); and where k is a thermal conductivity of the fluid [W/m.K].

The following formula is used to get the convective heat transfer coefficient, [1].

$$h=\frac{q}{A\,(\Delta T)} \quad (10)$$

where, q is the heat flow rate of the fuel (W), A is the heat transfer area(m^2); and temperature difference ΔT(K).

4.2.4 Set the Border and the Starting Conditions

On the borders of the flow domain, flow, thermal, and turbulence variables should be provided. All solids and liquids in the simulation should have their material qualities stated. If the boundary and beginning conditions at the CFD level are not provided in the validation problem or if they must be imposed in the application problem, they should be appropriate and their sensitivity should be assessed later. The commercial CFD code Ansys Fluent chooses a few physical models that are coherent with the meshing: It is decided to use the Reynolds-Averaged Navier-Stokes (RANS) model, specifically the k-turbulent model, which entails adding a further turbulent viscosity to the momentum and energy equations. The momentum equation and the energy equation are not connected. The turbulent viscosity is calculated using the turbulent energy per unit mass, k-, and the dissipation per unit mass. Each of these two terms is the answer to a transport equation. The wall law model is applied, which is a two-layer all y^+ treatment (Figure 14). The non-dimensional wall-adjacent grid height, which depends on the fluid characteristics and the skin friction coefficient, is simply the y^+ value (equation 11).

$$y^+=\frac{\rho u_{x\Delta y}}{\mu} \quad (11)$$

Where, y^+ is a non-dimensional measurement of distance from a wall,ρ=density of the fluid, u_x is the velocity of the fluid in *x*-direction and Δy is the distance of the first node from the wall and μ is fluid viscosity.

For coarser meshes ($y^+ \geq 30$), ANSYS Fluent offers the option to use the normal wall treatment approach; for low wall y^+ meshes ($y^+ \leq 1$), it offers an improved wall treatment option. The value of y+ must fall between 1 and 30 to be employed in the current simulation's k-ε model with an enhanced wall function technique. The y^+ distribution of the mesh created for the computation using the enhanced wall function method and the k-ε model is displayed in Figure 14. It can be observed that y^+ values range from <1 to ~5. As a result, the values of y^+ satisfy the conditions of the turbulent model used in this investigation.

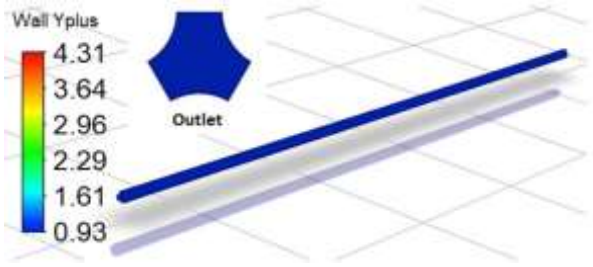

Fig. 14: y^+ value over wall fuel rod for polyhedral mesh, [43]

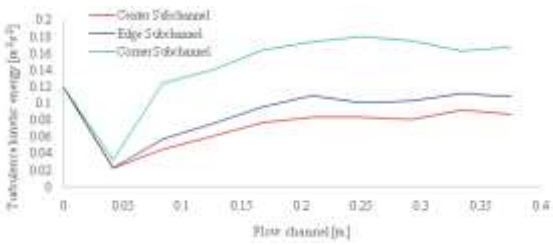

Fig. 15: Turbulence kinetic energy along flow channel in 3 sub-channels

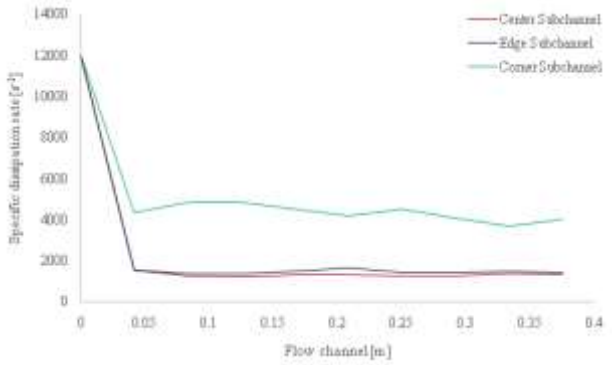

Fig. 16: Specific dissipation rate along flow channel in 3 sub-channels

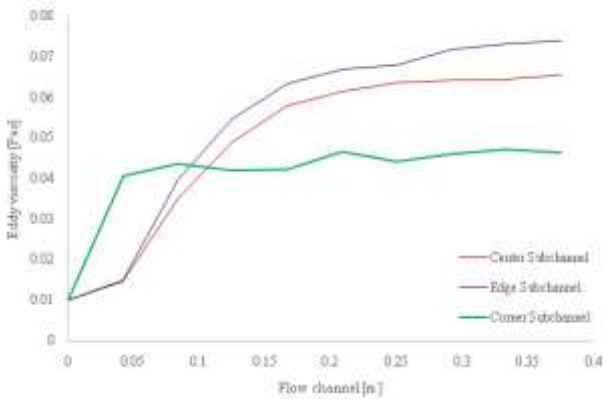

Fig. 17: Eddy viscosity along flow channel in 3 sub-channels

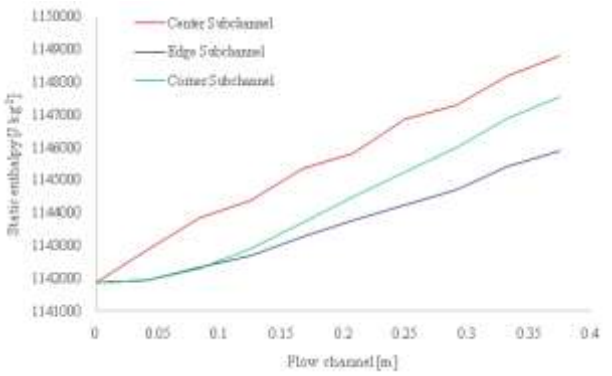

Fig. 18: Static enthalpy along flow channel in 3 sub-channels

5 Results and Discussion

5.1 Turbulence Kinetics

Due to the high Reynolds number, coolant water flow that is moving axially is turbulent. The flow characteristics and temperature distribution of the fluid are significantly influenced by turbulent features such turbulence kinetic energy, specific dissipation rate, eddy viscosity and static enthalpy. According to Figure 15 and Figure 16 the corner sub-channel has a greater concentration of all features than the inner or edge sub-channels. Additionally, compared to the center and edge sub-channels, the corner sub-channel has a somewhat higher rate of specific dissipation. And according to Figure 17 the corner sub-channel has a lower concentration of all features than the center or edge sub-channels. Additionally, compared to the center and edge sub-channels, the corner sub-channel has a somewhat lower eddy viscosity. Figure 18 depicts that the static enthalpy of the corner sub-channel is higher than edge sub-channel as well as lower than the center sub-channel.

5.2 Velocity Distribution

The velocity distribution along three sub-channels is depicted in Figure 19 based on flow channel. 5.66 ms^{-1} is the constant inlet velocity. All of the sub-channel velocities sharply increase to 10.4% of the overall length. Then, a progressive increase in velocity was seen along the center and edge sub-channels. However, as seen in Figure 15 and Figure 16 the higher turbulence kinetic energy and specific dissipation rate causes the velocity of the corner sub-channel to drop. According to Figure 17, lower eddy viscosity is another cause of the velocity of the corner sub-channel drop. This results from the formation of huge eddies and their subsequent splitting into smaller eddies. Internal fluid friction increases in this area more than in other sub-channels throughout these processes, which causes flow velocity in the corner to drop.

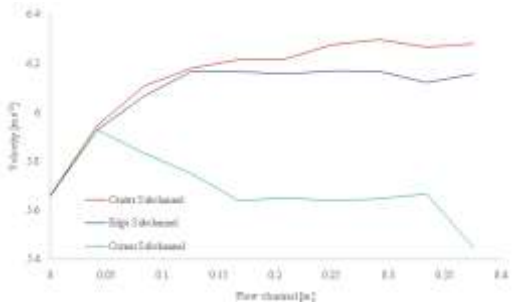

Fig. 19: Velocity distribution along flow channel in 3 sub-channels

5.3 Temperature Distribution

Figure 20 displays the temperature distribution along the flow channel in 3 sub-channels. The temperature distribution was measured using the reference line that ran along the axial direction of the graph, which showed that the temperature in the inlet was maintained at 571.2 K throughout the process. The temperature down the path went up because the uniform heat flux of the fuel rod was distributed evenly across the sub-channel. The 2.3 K

rise in temperature represents the 15% increase in height of the active fuel rod. A comparison was made between the analytical solution to the temperature problem and the data that was generated numerically. The error percentage was found to be almost 0.18 %.

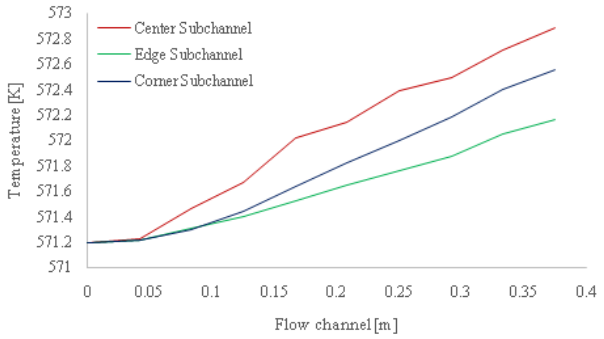

Fig. 20: Temperature distribution along flow channel in 3 sub-channels

5.4 Pressure Drop Variation

The average pressure at the entrance is 16.2 MPa, and the outflow pressure is constant at 16.19 MPa. Here, the use of water as a coolant result in a total pressure drop of 12.9 kPa, 13.7 kPa, and 54.2 kPa in the center, edge, and corner sub-channels, respectively. Figure 21 represents the variation of pressure drop along flow channels in 3 sub-channels. Viscosity shear stresses in the fluid and turbulence along the inner walls of the flow channel prevent fluid from flowing through the flow channel. The formula is as follows, [1], [66]:

$$\Delta p_{friction} = f \frac{L}{D_h} \frac{\rho V_m^2}{2}$$

Where, ΔP = pressure loss (Pa) f =friction coefficient, = length of the flow channel (m), D_h = hydraulic diameter (m) ρ = density (kg/m^3), and V_m = velocity (m/s).

There is a drop in pressure in the sub-channel along the axial direction of the channel. Pressure decreases as a result of eddies or vortices forming within the turbulent flow. These eddies are produced by the mixing of fluid particles traveling at different speeds and directions, which can result in pressure pockets inside the flow. More turbulence from these eddies increases the overall pressure drop in the axial direction. The subchannel's pressure distribution is described in Figure 21.

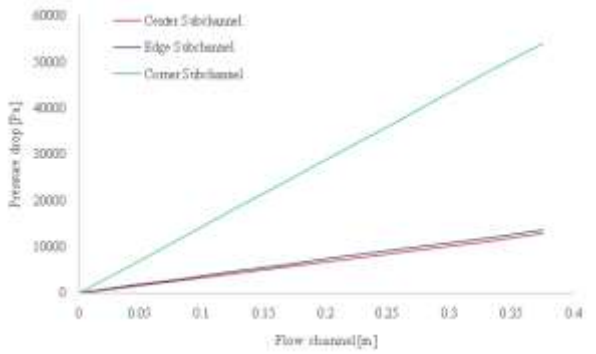

Fig. 21: Pressure drop along the axial distance of the sub-channel in 3 sub-channels

5.5 Reynolds Number Variation

According to equation (12), velocity and Reynolds number are related. The hydraulic diameter, D_h, which varies in the three sub-channels, determines the Reynolds number. D_h of the interior sub-channel was found to be 6 mm, for the edge sub-channel to be 10 mm, and for the corner sub-channel to be 4 mm using equation (12). The change in Reynolds number is depicted in Figure 22. Greater Reynolds numbers in the edge sub-channel indicate that convective heat transfer occurs here more frequently than in the other two sub-channels. The length of the sub-channel must be fixed for adequate heat removal while taking into account the bare minimum length required to get a fully developed Reynolds number. Reynolds number peaks in the corner sub-channel in $5D_h$ and steadily drops throughout the flow channel. This implies that the convective heat transfer in this sub-channel is decreasing, but the static fluid enthalpy in the corner sub-channel is growing, as illustrated in Figure 18. Therefore, there is a chance that nucleate boiling (DNB) will develop at the corner sub-channel for low Reynolds number and high static enthalpy of fluid, [1]. A two-phase flow might develop as a result of nucleate boiling, which would reduce the convective heat transfer coefficient.

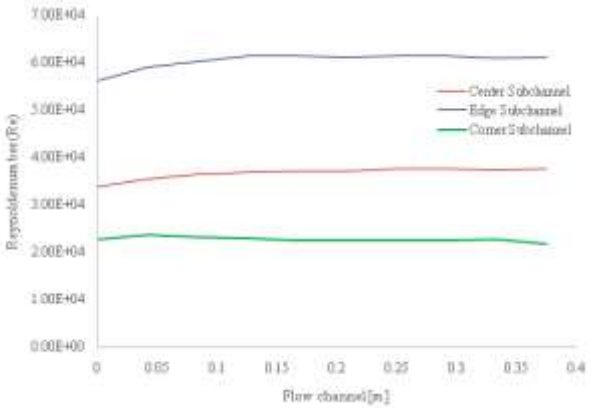

Fig. 22: Reynolds number (Re) variation along flow channel in 3 sub-channels

5.6 Friction Factor

The velocity in various sub-channels is used to compute the friction factor. Figure 23 illustrates how the friction factor varies along three sub-channels of the flow channel. Due to a larger coolant flow area, the friction factor is higher in the edge sub-channel. Interestingly, the additional eddy viscosity in the flow area of the coolant sub-channel causes its friction factor gradient along the flow channel to be higher than that of the interior sub-channel while having a smaller flow area. The following formula can be used to determine the friction factor (f):

$$f=(\tau_w / (0.5 * \rho * U^2))*L/D$$

Where, τ_w is the wall shear stress, ρ is the fluid density, L is the length and D is the hydraulic diameter. The velocity of the free stream is U.

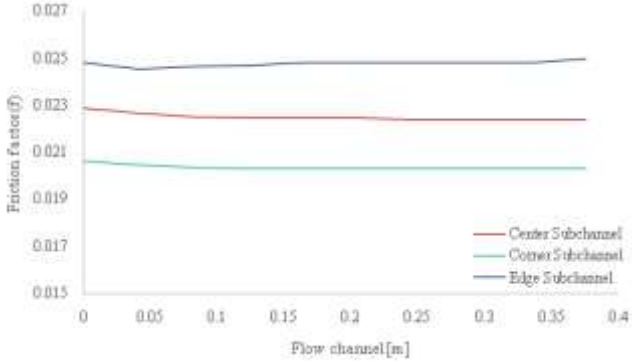

Fig. 23: Variation of friction factor along flow channel in 3 sub-channels

5.7 Nusselt Number and Convective Heat Transfer Coefficient Variation

The Nusselt number variation along flow channels in 3 sub-channels is depicted in Figure 24. And the convective heat transfer coefficient variation of the center sub-channel along the flow channel is depicted in Figure 25.

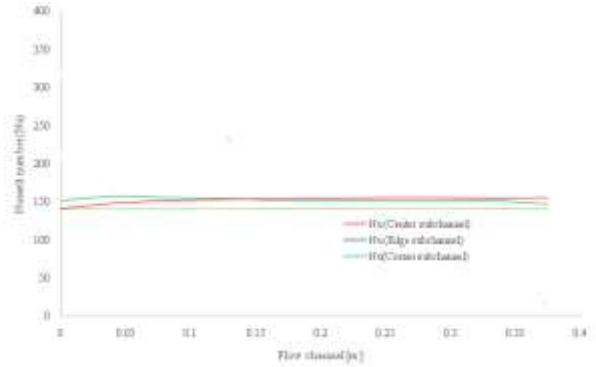

Fig. 24: Nusselt number variation along flow channel in 3 sub-channels

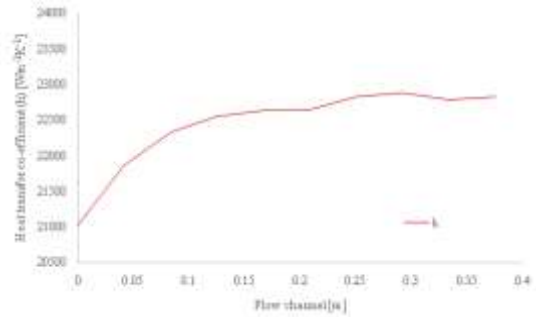

Fig. 25: Heat transfer coefficient variation of center sub-channel

5.8 Validation

Validation is very important for any simulation model. For this purpose, in this study validation is done with another model. In this study k-omega SST model is done for all simulating working processes and validation is done by the k-epsilon model. That is shown in Figure 26, Figure 27 and Figure 28. The velocity, temperature, and pressure drop variation between k-omega SST and k-epsilon model is shown in Figure 26, Figure 27 and Figure 28 respectively. In addition, there is a slight change in the value of velocity, temperature, and pressure drop along the flow channel but the nature of the graph is almost the same between the two models.

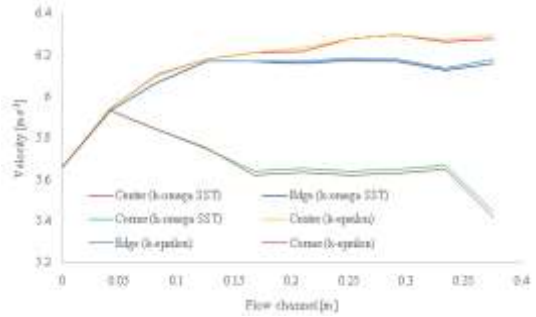

Fig. 26: Validation of velocity

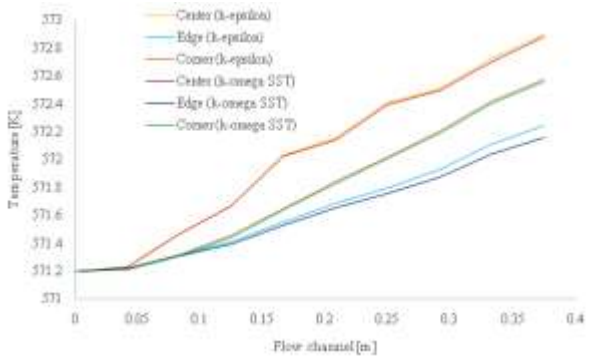

Fig. 27: Validation of temperature

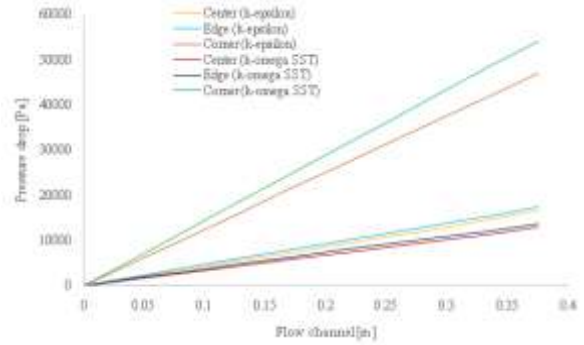

Fig. 28: Validation of pressure drop

6 Future Directions

According to the literature review on the topic, it is also possible to model numerous experimental studies on turbulent mixing under various fluid conditions by using sub-channel and CFD analysis. As a result, trustworthy CFD mixing forecasts can be made. Thus, to reliably estimate the safety margins of the nuclear reactor core, the study will focus on the following sub-channel analysis gap areas:

a. better heat transfer and mixing correlation thermal hydraulic sub-channel analysis tools;
b. enhance code to handle numerous sub-channels and fuel rod configurations;
c. CFD code to incorporate validation and verification of previous research studies; and
d. Create a thermal hydraulic test facility (Figure 29) on a laboratory scale, [78], [80] to validate CFD models and offer technical assistance to NPP operators.

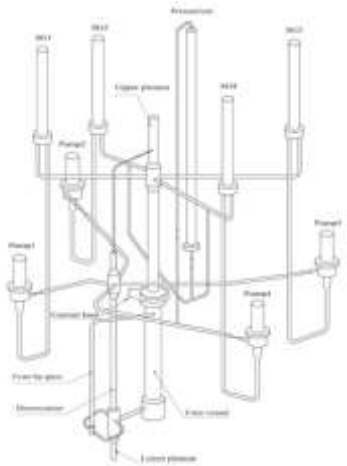

Fig. 29: General view of the integrated thermal hydraulic test facility, [80].

7 Conclusions

Sub-channel analysis algorithms are frequently employed in nuclear reactor core thermal-hydraulic analyses to calculate various thermal-hydraulic safety margins. The safety margins and operating power limits of the nuclear reactor core under various key system variables, such as system pressure, coolant input temperature, coolant flow rate, and thermal power and its distributions, are the primary parameters for sub-channel analysis. Due to the intricacy of the rod bundle shape, the range of turbulent scales, and the resource limitations, a full-scale computational fluid dynamic (CFD) simulation of a nuclear reactor core is time- and labor-intensive to complete. Knowledge of forced convective heat transfer within sub-channels formed between multiple nuclear fuel rods or heat exchanger tubes, not only in the fully developed regime but also in the developing regime or laminar flow regime, is necessary for the development of new procedures in nuclear reactor safety aspects and optimization of modern nuclear reactors, [66], [67], [68].

With the use of ANSYS's turbulence model, the three sub-channels such as center, corner, and edge using three fuel rods have been analyzed. The effects of turbulent flow on temperature distribution, velocity variance, pressure drop, friction factor, Reynolds number, etc. have been examined for different sub-channels of VVER-1200 via a rod bundle with three sub-channels that are a good representation of those employed in the VVER-1200. A 311 rod bundle is projected to require around 500 times as many computing cells as a 3 rod bundle with 700 mm lengths. As a result, there will be a total of one billion cells, or around 500 times the number of three rod bundles. The necessary computer memory will be 500 times larger, or 1000 GB RAM. The development of parallel CFD software and structural mesh-generating tools for rod bundles is the focus of research activities to address these issues. The study provides valuable information for future research and practical applications in the field of nuclear power plants.

In terms of the model's application, the suggested models can be duplicated and used in other fields, such as air conditioning, heating, cooling, and particularly hydraulic turbines. This study adds to the body of knowledge regarding the performance simulation of thermal hydraulics for different kinds of nuclear reactors.

As it is a new type of power plant (VVER-1200), more research is needed to understand its thermal hydraulics behavior and for upgrading its

operation capacity. In conclusion, despite significant developments in CFD over the past couple of decades that have made it possible to perform thermal hydraulics analysis along with neutronics, further study is needed to develop suitable coupling codes such as SuperMC and SUBCHANFLOW, [28], [65], [70], [71], [72], [73]. [74], [78]. Future research on the full-dimensional fuel bundle model is intended to give in-depth information on the characteristics of liquids and apply the findings to the operation and safety analyses of VVER-1200 nuclear power plants that will be constructed in Bangladesh.

Acknowledgments:
The author would like to thank everyone who provided assistance, inspiration, and support. As some of them might not be alive to witness the outcome of their encouragement, we have chosen not to name them all. But, we do hope that they can at least read this acknowledgment, wherever they may be.

References:

[1] Todreas, N. E., and Kazimi, M. S. (2011). Nuclear systems volume I and II: Thermal hydraulic fundamentals. CRC press.

[2] Mollah, A. S., Sabiha Sattar, M. A, Hossain, A Z M Salahuddin and S. Khan, Review and analysis of environmental impacts of different energy technologies: clean environment from nuclear energy, MIST Journal of Science and Technology, Vol. 4(1), 1, (2016).

[3] World Energy Outlook, International Energy Outlook, OECD/IEA, 2010 International Energy Agency

[4] Reference Data Series, IAEA-RDS-2/36 2016 Edition, Nuclear Power Reactors in the World, [Online]. https://www-pub.iaea.org/MTCD/Publications/PDF/RDS_2-36_web.pdf (Accessed Date: January 23, 2024).

[5] Nuclear Power in the World Today, [Online]. https://world-nuclear.org/information-library/current-and-future-generation/nuclear-power-in-the-world-today.aspx (Accessed Date: January 18, 2024).

[6] Zohuri, B., and Fathi, N. (2015). Thermal-hydraulic analysis of nuclear reactors, New York: Springer.

[7] Guan Heng Yeoh, Thermal hydraulic considerations of nuclear reactor systems: Past, present and future challenges, Exp. Comput. Multiph. Flow 1, 3–27 (2019).

[8] Sha, W. T. An overview of rod-bundle thermal-hydraulic analysis. Nucl. Eng. Des., 62: 1–24 (1980).

[9] Yadigaroglu, G., Anderani, M., Dreier, J., and Coddington, P. Trends and needs in experimentation and numerical simulation for LWR safety. Nucl.Eng. Des.221,205–223 (2003).

[10] El-Wakil, M.M., 1981. Nuclear Heat Transport. The American Nuclear Society.

[11] Heat Equation - Heat Conduction Equation, Definition, [Online]. https://www.nuclear-power.com/nuclear-engineering/heat-transfer/thermal-conduction/heat-conduction-equation/ (Accessed Date: January 18, 2024).

[12] D. Bestion and C. Morel. “Balance equations”. In: Thermal-Hydraulics of Water Cooled Nuclear Reactors. Journal Abbreviation: Thermal-Hydraulics of Water Cooled Nuclear Reactors. Dec. 2017, pp. 167–244. ISBN: 978-0-08-100662-7. doi: 10.1016/B978-0-08-100662-7.00005-1.

[13] White, F. M. Fluid Mechanics, fourth ed., McGraw-Hill, New York, 1999.

[14] Patankar, S. V. Numerical Heat Transfer and Fluid Flow, McGraw-Hill, New York, (1980).

[15] Munson, B.R., Young, D.F., and Okiishi, T.H. (2005). Fundamentals of Fluid Mechanics (5th ed.). Wiley.

[16] Çengel, Y.A. and Ghajar, A.J. (2014). Heat and Mass Transfer: Fundamentals and Applications (5th ed.). McGraw-Hill.

[17] Ferziger, J. H. (2002). Computational methods for fluid dynamics, 3rd Ed., Springer, USA.

[18] D’Auria, F., Upendra S. and Rohatgi. A. Historical perspective of nuclear thermal hydraulics. Tech. rep. BNL-200033-2018-BOOK.Woodhead Publishing, Jan. 2017.doi: 10.1016/B978-0-08-100662-7.00002-6.

[19] Reventos, F. Parameters and concepts, Chapter 3, In Book-Thermal-Hydraulics of Water Cooled Nuclear Reactors, Woodhead Publishing, 2017.

[20] Schultz, R. R. Role of thermal-hydraulics in nuclear power plants: Design and safety, Chapter 4, In Book - Thermal-hydraulics of Water Cooled Nuclear Reactors, Woodhead Publishing, (2017).

[21] Saha, P., Aksan, N., Andersen, J., Yan, J., Simoneau, J.P., Leung, L., Bertrand, F., Aoto, K. and Kamide, H. Issues and future direction

of thermal-hydraulics research and development in nuclear power reactors. Nucl. Eng. Des. 264, 3–23 (2013).

[22] Cheng J.P, Yan L.M, Li F.C. CFD simulation of a four-loop PWR at asymmetric operation conditions. Nuclear Engineering and Design. 300:591-600 (2016).

[23] H. Ganjiani and B. Firoozabadi, Three Dimensional Simulation of Turbulent Flow in 3 Sub-channels of a VVER-1000 Reactor", Transaction B: Mechanical Engineering, Vol. 17, No. 2, pp. 83-92 (2010).

[24] Shojaa Ayed Aljasar, Oleg. Yu Dolmatov, Muhammad Saqib and Yubin Xu, Analysis of the coolant flow in sub-channels of the vver-1000 reactor by CFD method, International Journal of Mechanical and Production Engineering Research and Development (IJMPERD) ISSN (P): 2249–6890; ISSN (E): 2249–8001 Vol. 10, Issue 2, 1419–1428(2020).

[25] Dinh Van Thin, P. L. Analysis of the fluid flow characteristics in subchannels of VVER-1000 reactor's fuel assemblies by CFD method. Nukleon, Vol. 189, 1-6 (2016).

[26] Tóth, S., and Aszódi, A. CFD analysis of flow field in a triangular rod bundle. Nuclear Engineering and Design, Vol. 31, 352-363 (2010).

[27] Talebi, S., and Valoujer, M. Thermal–hydraulic performance analysis of a sub-channel with square and triangle fuel rod arrangements using the entropy generation approach. Nuclear Science and Techniques, Vol. 28, 149-156 (2017).

[28] Wu, Y., Song, J., Zheng, H., Sun, G., Hao, L., Long, P., Hu, L., FDS Team. CAD based Monte Carlo program for integrated simulation of nuclear system SuperMC. Ann. Nucl. Energy 82, 161–168 (2015).

[29] Safikhani, S. M., Ebrahimnejad, S., and Mohammadi, H. Thermal-hydraulic analysis of sub-channels in VVER-1000 nuclear reactor fuel assemblies. Progress in Nuclear Energy, 94, 65-76 (2017).

[30] Tandian, N.P.; Umar, E.; Hardianto, T.; and Febriyanto, C. Experimental study of natural convective heat transfer in a vertical hexagonal subchannel. AIP Conf. Proc. 1448, 252–260 (2012).

[31] Liu, B.; He, S.; Moulinec, C.; Uribe, J. Sub-Channel CFD for nuclear fuel bundles. Nucl. Eng. Des. 355, 110318 (2019).

[32] Chen, J.; Gu, H.; and Xiong, Z. A circumferentially non-uniform heat transfer model for sub-channel analysis of tight rod bundles. Ann. Nucl. Energy, 121, 50–61 (2018).

[33] Cheng Z, and Rao Y. Strategies for developing sub-channel capability in an advanced system thermal-hydraulic code: a literature review. AECL Nuclear Review. 4(1):23-41 (2015).

[34] Doster, M.D. and Jackson, T.A. Sub-channel Analysis. Nuclear Engineering and Design, Vol.278, 11-25 (2014).

[35] Durakovic, L., and Tucakovic, A. R. CFD analysis of sub-channel and single-phase coolant flow in VVER-1200 fuel assembly. Nuclear Engineering and Design, 315, 307-319 (2017).

[36] Liu, B., He, S., Moulinec, C., & Uribe, J. Sub-channel CFD for nuclear fuel bundles. Nuclear Engineering and Design, Vol. 355, 110318 (2019).

[37] Anil Kumar Sharma, A. M. A review of sub-channel thermal hydraulic codes for nuclear reactor core and future directions. Nuclear Engineering and Design, Vol. 332, 329-344 (2018).

[38] Chih-Hung, L., Cheng-Han, Y., and Yuh-Ming, F. CFD investigating the flow characteristics in a triangular-pitch rod bundle using Reynolds stress turbulence model. Annals of Nuclear Energy, Vol. 31, pp. 357-364 (2014)

[39] Liu, Y. M. CFD evaluation of turbulence models for flow simulation of the fuel rod bundle with a spacer assembly. Applied Thermal Engineering, Vol 40, 389-396 (2012).

[40] Moorthi, A., Sharma, A., and Velusamy, K. A review of sub-channel thermal hydraulic codes for nuclear reactor core and future directions. Nuclear Engineering and Design, Vol. 332, 329-344 (2019).

[41] Hassan, Y. An overview of computational fluid dynamics and nuclear applications, Chapter 12, In Book- Thermal-Hydraulics of Water Cooled Nuclear Reactors, Woodhead Publishing, 2017.

[42] Karachevtsev, A. V., Khoruzhii, O. V., and Putilov, A. V. The fuel assembly of the VVER-1200 reactor: design features and analysis of the fuel rod behavior. Nuclear Engineering and Technology, Vol. 50(3), pp. 382-392 (2018).

[43] Ahmed, F., M.A. Abir, PK Bhowmik, V Deshpande, A.S. Mollah, and D Kumar, Computational assessment of the thermo-

hydraulic performance of Al_2O_3-water nanofluid in hexagonal rod-bundles sub-channel, Progress in Nuclear Energy, Vol. 135, 103700 (2021).

[44] Ahmed, F., Md Atrehar Abir, P.K. Bhowmik, V. Deshpande and A. S. Mollah, Thermohydraulic performance of water mixed Al_2O_3, TiO_2 or graphene-oxide nanoparticles for nuclear fuel triangular sub-channel, Thermal Science and Engineering Progress, Vol. 24, 100929, (2021).

[45] Moorthi, A., Anil Kumar Sharma, and K. Velusamy, A review of sub-channel thermal hydraulic codes for nuclear reactor core and future directions, Nuclear Engineering and Design 332, 329–344, (2018).

[46] Yan, J., He, J., and Huo, Z. Experimental and numerical study on the thermal-hydraulic behavior of the VVER-1200 fuel sub-channel. Annals of Nuclear Energy, 97, 182-189 (2016)

[47] Mahfuzul H. R., Asma UlHusna, and Israt Jahan Tonny, Thermal hydraulic analysis in triangular sub-channel for 3MW Triga Mark II research reactor by using Ansys software, B.Sc. Engineering Thesis (Supervised by Prof. Dr. A. S. Mollah), Department of Nuclear Science and Engineering, Military Institute of Science and Technology, Dhaka, Bangladesh, March 2022.

[48] Mosaddak A. Z., Shamsul Arefin Shibly, and Md. Imam Mehedi. Thermal-hydraulic analysis for different sub-channels of VVER-1200 reactor with al_2o_3-water nanofluid, BSc Engg. thesis (Supervised by Prof. Dr. A. S. Mollah), Department of Nuclear Science and Engineering, Military Institute of Science and Technology, Dhaka, Bangladesh, February 2023.

[49] Summary Review on the Application of Computational Fluid Dynamics in Nuclear Power Plant Design, IAEA NUCLEAR ENERGY SERIES No. NR-T-1.20, (2022).

[50] Sharma, A. K., Moorthia, A., &Velusamy, K. A review of sub-channel thermal hydraulic codes for nuclear reactor core and future directions. Nuclear Engineering and Design, Vol. 45, 329-344 (2018).

[51] Efrizon Umar, Nathanael Panagung Tandian, Ahmad Ciptadi Syuryavin, Anwar Ilmar Ramadhan and JokoHadi Prayitno. CFD Analysis of Convective Heat Transfer in a Vertical Square Sub-Channel for Laminar Flow Regime, Fluids 7, 207(2022) https://doi.org/10.3390/fluids7060207.

[52] Bestion D. Chapter 11 - The structure of system thermal-hydraulic (SYS-TH) code for nuclear energy applications". en. In: Thermal-Hydraulics of Water Cooled Nuclear Reactors. Ed. by Francesco D'Auria.Woodhead Publishing, Jan. 2017, pp. 639–727.

[53] TRACE. TRACE V5.1051 Theory Manual. Washington DC: Division of Safety Analysis Office of Nuclear Regulatory Research U. S. Nuclear Regulatory Commission; 2016.

[54] Bestion, D., Barre, F., Faydide, B., 1999. Methodology, status and plans for development and assessment of CATHARE code. In: Proc. of Int. Conf. OECD/CSNI, Annapolis, USA, November 5–8, 1999.

[55] VIPRE-01, Numerical Advisory Solutions, [Online]. https://www.numerical.com/software/vipre/vipre-01 (Accessed Date: January 18, 2024).

[56] RETRAN-3D - A Program for One-Dimensional Transient Thermal-Hydraulic Analysis of Complex Fluid Flow Systems Volume 3: User's Manual", [Online]. https://www.epri.com/research/products/NP-7450-V3R3 (Accessed Date: January 18, 2024).

[57] Burwell, M.J.; Lerchl, G.; Miro, J.; Teschendorff, V.; Wolfert, K. The thermal hydraulic code ATHLET for analysis of PWR and BWR systems, Fourth international topical meeting on nuclear reactor thermal-hydraulics (NURETH-4). Proceedings. Vol. 21989

[58] Escalante J, Marcello V, Espinoza V, Perin Y. Application of the ATHLET/COBRA-TF thermal-hydraulics coupled code to the analysis of BWR ATWS. Nuclear Engineering and Design. 321:318-327 (2017).

[59] Salko, R. K. and M. N. Avramova, "COBRA-TF subchannel thermal-hydraulic code (CTF) theory manual," Pennsylvania State University, CASL-U-2015-0054-000, State College, 2015.

[60] RELAP5 code development Team, "RELAP5/MOD3 Code Manual", Idaho National Engineering Laboratory, 1995.

[61] Lee S.Y., Jeong J.J., Kim S-H, Chang SH. COBRA/RELAP5: a merged version of the COBRA-TF and RELAP5/MOD3 codes. Nuclear Technology. 1992, 99:177-186.

[62] FLOW-3D, [Online]. https://www.flow3d.com/ (Accessed Date: January 18, 2024).

[63] Runchal A, Sagar B. "PORFLOW: A Multifluid Multiphase Model for Simulating Flow, Heat Transfer, and Mass Transport in Fractured Porous Media," Nuclear Regulatory Commission, NUREG/CR--5991; CNWRA--92–003 ON: TI93008514. Washington, DC, U.S.: U.S. Department of Energy, Office of Scientific and Technical Information; 1993.

[64] Toumi I, Bergeron A, Gallo D, Royer E, Caruge D. FLICA-4: a three-dimensional two-phase flow computer code with advanced numerical methods for nuclear applications. Nuclear Engineering and Design. 200(1–2), 139-155 (2000).

[65] Louhanrong Yu, Lei Wang, Chao Liu, Bin Wu, Jing Song, and Yican Wu, Development and testing of a coupled SuperMC and SUBCHANFLOW code for LWR simulations, Annals of Nuclear Energy 144 (2020) 107465.

[66] Ansys, Engineering Simulation Software, [Online]. https://www.ansys.com/ (Accessed Date: January 18, 2024).

[67] Hastuti, E. P., Yamaguchi, A., and Takata, T. Comparative study of turbulence models on PWR fuel bundle thermal hydraulics using FLUENT code, Vol. 9, pp. 4-6 (2008).

[68] OpenFOAM, [Online]. https://www.openfoam.com/ (Accessed Date: January 18, 2024).

[69] Mohamed Y.M., Mohsen, Abdelfattah Y. Soliman, and Mohamed A.E. Abdel-Rahman, Thermal-hydraulic and solid mechanics safety analysis for VVER-1000 reactor using analytical and CFD approaches, Progress in Nuclear Energy, Volume 130, 103568 (2020),

[70] Wu Y, Song J, Zheng HQ, CAD-based Monte Carlo program for integrated simulation of nuclear system SuperMC. Annals of Nuclear Energy 82: 161–168 (2015).

[71] Wang, L., He, P., Sun, G., Hao, L., Song, J., Research of SuperMC and Fluent coupling simulation based on the parametric-surface-represented entity clipping method. In: Proceedings of PHYSOR 2018 Conference, Cancun, Mexico (2018).

[72] Kanglong Zhang, The multiscale thermal-hydraulic simulation for nuclear reactors: A classification of the coupling approaches and a review of the coupled codes, Int J Energy Res. 44:3295–3315 (2020).

[73] Lin Sun, Minjun Peng, Genglei Xia, Xuesong Wang and Mingyu Wu, Development and Validation of Multiscale Coupled Thermal-Hydraulic Code Combining RELAP5 and Fluent Code, Frontiers in Energy Research 8 (2021), doi: 10.3389/fenrg.2020.613852.

[74] Bousbia-Salah A, and D'Auria F. Use of coupled code technique for best estimate safety analysis of nuclear power plants. Progress in Nuclear Energy, 49(1):1-13 (2007).

[75] Zerkak O, Kozlowski T, Gajev I. Review of multi-physics temporal coupling methods for the analysis of nuclear reactors. Annals of Nuclear Energy.84:225-233 (2015).

[76] Yadigaroglu G. Computational fluid dynamics for nuclear applications: from CFD to multi-scale CMFD. Nuclear Engineering and Design. 235(2–4):153-164 (2005).

[77] Kazuo Ikeda, CFD application to advanced design for high-efficiency spacer grid, Nuclear Engineering and Design, Volume 279, 73-82, 2014, https://doi.org/10.1016/j.nucengdes.2014.02.013.

[78] Mollah, A. S. Current research topics of the nuclear thermal-hydraulics analysis, Lecture note on NE305: Nuclear Reactor Thermal Hydraulics (Level 3, Term 1, March 2023), Department of Nuclear Science and Engineering, Military Institute of Science and Technology, Dhaka, Bangladesh.

[79] IAEA Status report 108 - VVER-1200 (V-491) (VVER-1200 (V-491).

[80] Toraj Khoshnevis, Jalil Jafari, and Mostafa Sohrabpour, Design, and analysis of a thermal hydraulic integral test facility for Bushehr nuclear power plant Pro. in Nucl. Energy, 51 (2009) 443–450, doi:10.1016/j.pnucene.2008.10.004.

Contribution of Individual Authors to the Creation of a Scientific Article (Ghostwriting Policy)

A. S. Mollah contributed towards the problem selection, the simulations, the analysis, wrote the paper and finally approved the final manuscript.

Sources of Funding for Research Presented in a Scientific Article or Scientific Article Itself

This research received no external funding.

Conflict of Interest

The author declares that no known competing financial interests or personal relationships could have appeared to influence the work reported in this paper**.**